Original Article

Low expression of PRTN3 regulates the progression of gastric cancer by inhibition of cell cycle and promotion of apoptosis

Haoyu Zhu[1#], Fei Wang[2#], Xinran Lu[1], Hao Wu[2], Chao Shi[3], Silvio Matsas[4], Renata D'Alpino Peixoto[5], Marcelo Porfirio Sunagua Aruquipa[6], Chong Tang[2], Shichun Feng[2]

[1]Department of Gastrointestinal Surgery, Nantong First People Hospital, Medical School of Nantong University, Nantong, China; [2]Department of Gastrointestinal Surgery, Nantong First People Hospital, Nantong, China; [3]Department of Pathology, Nantong First People Hospital, Nantong, China; [4]Centro de Estudos e Pesquisas de Hematologia e Oncologia (CEPHO), Santo André, SP, Brazil; [5]Department of Medical Oncology, BC Cancer Agency, Vancouver, BC, Canada; [6]Department of Gastrointestinal Oncology, Oncoclinicas, São Paulo, SP, Brazil

Contributions: (I) Conception and design: H Zhu; (II) Administrative support: S Feng; (III) Provision of study materials or patients: F Wang, C Shi; (IV) Collection and assembly of data: X Lu, H Wu; (V) Data analysis and interpretation: C Tang; (VI) Manuscript writing: All authors; (VII) Final approval of manuscript: All authors.

[#]These authors contributed equally to this work.

Correspondence to: Chong Tang, MS; Shichun Feng, MS. Department of Gastrointestinal Surgery, Nantong First People Hospital, No. 666 Shengli Road, Nantong 226001, China. Email: 15051273108@163.com; fsc2200@126.com.

Background: Proteinase 3 (PRTN3) has been linked to the progression of different cancer types. In this study, the expression and cell biological function of PRTN3 were investigated in gastric cancer (GC) to assess its role in GC progression.

Methods: The PRTN3 levels in 20 pairs of GC tissues were detected via quantitative real-time reverse transcription polymerase chain reaction (qRT-PCR) and Western blotting, while immunohistochemical staining was used to assess the PRTN3 levels in 47 GC tissue samples. The effects of stable lentivirus-mediated PRTN3 knockdown on GC cell proliferative, cell cycle, and apoptotic activity were evaluated using Cell Counting Kit-8 (CCK-8) and colony formation assays, nude mouse models, and flow cytometry.

Results: Elevated levels of PRTN3 messenger RNA (mRNA) and protein were noted in GC tissues, mostly in the cytosol. High PRTN3 levels were positively correlated with GC tumor N staging. *In vitro* knockdown of PRTN3 suppressed cell cycle progression, promoted apoptotic induction, and decreased the concentrations of cell cycle-associated proteins (cyclin D1, CDK4, and CDK6) and apoptosis-related Bcl-2 while inducing the upregulation of Bax. Downregulation of PRTN3 inhibited GC cell growth both *in vitro* and in mouse models.

Conclusions: Our study found that high expression of PRTN3 is associated with GC tumor N staging. And PRTN3 silencing could regulate GC progression by inhibiting the cell cycle and promoting apoptosis in GC cells, which could be a potential target for GC diagnosis and treatment.

Keywords: Proteinase 3 (PRTN3); gastric cancer (GC); proliferation; cycle; apoptosis

Submitted Jan 16, 2025. Accepted for publication Feb 13, 2025. Published online Feb 26, 2025.
doi: 10.21037/tcr-2025-153
View this article at: https://dx.doi.org/10.21037/tcr-2025-153

Introduction

Gastric cancer (GC) is a prevalent malignancy that remains the fifth most common and third deadliest cancer in the world (1). GC is often difficult to detect in its early stages owing to an absence of reliable symptoms, and it is also associated with high rates of metastasis and unfavorable patient prognosis. GC is often only diagnosed at a relatively advanced stage (2). Treatment approaches including radiotherapeutic, immunotherapeutic, targeted, surgical treatment and chemotherapeutic interventions can all

achieve some degree of efficacy in GC management (3), but patients with advanced GC continue to face a poor prognosis (4). Thus, it is vital to establish new biomarkers than can accurately diagnose GC and detect metastasis at an early stage, thereby enabling more effective and tailored management strategies to improve patient prognosis.

The neutral serine protease, proteinase 3 (PRTN3), is produced primarily by neutrophils and has a role in removing pathogenic microbes both intracellularly and extracellularly (5). In hematological diseases, PRTN3 levels have been linked to an increased risk of antineutrophil cytoplasmic antibodies (6). A report has also noted that PRTN3 is associated with oncogenic progression, where murine myeloid leukemia was suppressed through reductions in PRTN3 activity (7). PRTN3 is also capable of promoting hepatocellular carcinoma development through a range of oncogenic mechanisms (8), and high expression of PRTN3 may attenuate the efficacy of bevacizumab in colorectal cancer (9). High PRTN3 levels have also been reported to be of value for the early diagnosis of GC (10). The mechanisms by which PRTN3 functions in GC, however, have yet to be studied at length.

This study investigated the regulatory significance of PRTN3 in GC progression. Elevated PRTN3 levels were observed in GC cells and tissues using quantitative real-time reverse transcription polymerase chain reaction (qRT-PCR) and Western blotting. The relationship between clinicopathological correlation and PRTN3 expression was assessed in selected patients with complete clinical information. AGS cells and BGC-823 cells with high PRTN3 expression were effectively transfected with lentiviral interference fragments, and the effect of PRTN3 knockdown on GC cell function was analyzed. It was found that PRTN3 downregulation blocked the cell cycle while promoting apoptosis in GC cells. Notably, it was demonstrated, both *in vivo* and *in vitro*, that low PRTN3 levels were associated with reduced GC cell growth. These findings support the biological and clinical relevance of PRTN3 in GC, suggesting its potential in diagnosing and treating GC. We present this article in accordance with the ARRIVE and MDAR reporting checklists (available at https://tcr.amegroups.com/article/view/10.21037/tcr-2025-153/rc).

Highlight box

Key findings

- Proteinase 3 (PRTN3) is highly expressed in gastric cancer (GC), mainly in the cytoplasm.
- Low expression of PRTN3 inhibited the proliferation of GC cells *in vivo* and *in vitro*, hindering the cell cycle process and promoting the apoptosis of GC cells.

What is known and what is new?

- Elevated levels of PRTN3 have been reported in early GC, but its regulatory mechanism has not been extensively investigated.
- PRTN3 is highly expressed in GC and correlates with GC tumor N staging, while down-regulation of PRTN3 expression inhibited the proliferation and cycle progression of GC cells, but promoted apoptosis of GC cells.

What is the implication, and what should change now?

- These results suggest that PRTN3 may be a potential target for the future diagnosis and treatment of GC.

Methods

Patients and samples

Tumor pathology specimens from 47 patients with GC who had undergone treatment at Nantong First People Hospital between March 1, 2023 and February 29, 2024 were analyzed. All of these tumor specimens were obtained surgically. None of these patients had undergone radiotherapy, immunotherapy, or neoadjuvant chemotherapy before sample collection. A tissue microarray (TMA) was used to analyze GC tumors and paracancerous tissues from these 47 patients. Clinical information was retrieved from the official medical records of the hospital. In addition, 20 tumor tissue samples were collected from cases who had been diagnosed at the same hospital between January 2023 and December 2023. The study was conducted in accordance with the Declaration of Helsinki (as revised in 2013). The study was approved by the Ethics Committee of Nantong First People Hospital (No. 2024KT182) and informed consent was taken from all the patients.

Cell culture and transduction

The HGC-27, MGC-803, BGC-823, MKN-45, AGS, and SGC-7901 GC cell lines, in addition to the GES-1 normal gastric mucosal cell line, were purchased from GeneChem (Shanghai, China). All cells were grown with 5% CO_2 in RPMI-1640 (cat. no. PM150110; Pricella, Shanghai, China) with 10% fetal bovine serum (FBS) (cat. no. C04001; HyClone, Logan, UT, USA) at 37 ℃ (11).

Lentiviral particles encoding short hairpin RNA (shRNA), including negative control shRNA (shNC)

and PRTN3-specific shRNA (shPRTN3), were prepared using GV 493 lentivirus particles (cat. no. GIEL0392716 GeneChem) (shPRTN3-#1: CCTGACTTCTTCACGCGGGTA; shPRTN3: CCTGATCTGTGATGGCATCAT; shPRTN3-#2: GCCACATAACATTTGCACTTT). AGS cells and BGC-823 cells were then transduced with the lentiviruses in six-well plates when 70–80% confluent. After 72 hours, stable cell lines selected with puromycin (2 μg/mL; cat. no. ST551; Beyotime Biotechnology, Shanghai, China) were used for analysis, with the PRTN3 knockdown efficiency verified by qRT-PCR and Western blotting.

qRT-PCR analysis

Total RNA from 20 pairs of tumor samples and GC cells were isolated using TRIzol (cat. no. 15596018CN; Thermo Fisher Scientific, Waltham, MA, USA), and complement DNA (cDNA) was prepared using the Prime script RT kit (cat. no. RR055A; Takara Bio, Kusatsu, Japan). All qRT-PCR analyses were conducted with the 7500/7500 Fast Real-Time PCR System (cat. no. 100048201; Thermo Fisher Scientific) under conditions identical to those reported previously (12). Primers, which were produced by Shanghai Bioengineering Genetics (cat. nos. 25030191 and 250261068; Shanghai, China), had the following sequences: forward PRTN3, 5'-ACAGCAGGACCAGCCAGTG-3'; reverse PRTN3, 5'-GAAGGTGACCACGGTGACATTG-3'; forward glyceraldehyde-3-phosphate dehydrogenase (GAPDH), 5'-AGAAGGCTGGGGCTCATTTG-3'; and reverse GAPDH, 5'-AGGGGCCATCCACAGTCTTC-3'. Analyses were completed in triplicate. Finally, the experimentally obtained cycle threshold (Ct) values of PRTN3 and GAPDH were analyzed via SPSS 19.0 (IBM. Corp., Armonk, NY, USA) for data analysis via the $2^{-\Delta\Delta Ct}$ normalization method.

Western blotting

For Wester blotting, RIPA buffer (cat. no. P0013B; Beyotime Biotechnology) was used to lyse cells and tumor tissues, and separating gels (concentration =10%; cat. no. PG112; Yarase Bio, Shanghai, China) made on glass plates were used to separate proteins via sodium dodecyl sulfate-polyacrylamide gel electrophoresis (SDS-PAGE). At a voltage of 90 V, we separated the proteins from the upper layer of gel to the lower layer of gel within 30 min; then at 120 V, we split the proteins from the lower layer of gel to the bottom of the gel within 60 min. Subsequently, in a 1-hour ice bath (300 mA), the separated proteins were transferred to polyvinylidene fluoride (PVDF) membranes (0.45 μm; cat. no. IPVH00010; Millipore, Billerica, MA, USA). After being blocked at room temperature with skimmed milk for 2 hours, the blots were treated (overnight at 4 ℃) with antibodies against PRTN3 (1:3,000; cat. no. ab133613; Abcam, Cambridge, UK), CDK6 (1:2,000; cat. no. 14052-1-AP; Proteintech), CDK4 (1:2,000; cat. no. 11026-1-AP, Proteintech), cyclin D1 (1:5,000; cat. no. 60186-1-Ig; Proteintech), BCl-2 (1:4,000; cat. no. 16026-1-AP; Proteintech), Bax (1:5,000; cat. no. 50352-1-AP; Proteintech), and GAPDH (1:10,000; cat. no. 60004-1-Ig; Proteintech). These antibodies were selected according to previous reports (13,14). The blots were then probed with anti-rabbit (1:10,000; cat. no. 66467-1-Ig; Proteintech) or anti-mouse immunoglobulin G (IgG) (1:10,000; cat. no. SA00001-1; Proteintech) for 1.5 hours. Finally, a Touch Imager (e-Blot, Shanghai, China) was used to visualize and analyze the PVDF membranes, and the images were quantified using ImageJ v. 1.45 (National Institutes of Health, Bethesda, MD, USA).

Cell Counting Kit-8 (CCK-8) and colony formation assays

AGS cells and BGC-823 cells (500/well) were grown in 96-well plates, and CCK-8 assays (cat. no. PF00004; Beyotime) were performed as directed, with cells being collected after 0, 24, 48, 72, and 96 hours and absorbance measured at 450 nm with a microplate reader (cat. no. E0227; Beyotime). In colony formation assays, AGS cells and BGC-823 cells (200/well) were grown in six-well plates in a 5% CO_2 incubator (Heracell 150i GP, Thermo Fisher Scientific) at 37 ℃ for 2 weeks until distinct colonies were visible under a microscope (E200 POL, Nikon, Japan) and then fixed with methanol (concentration ≥99.5%; cat. no. 10014118; Sinopharm Chemical Reagent Co., Shanghai, China) and stained using 1% crystal violet (cat. no. V5265; Merck, Germany). Numbers of colonies in each well were counted, and analyses were performed in triplicate.

Mouse model experiments

Twelve 4-week-old male nude BALB/c mice, obtained from the Animal Experiment Center of Nantong University,

were placed in specific pathogen-free (SPF) conditions and randomized into two groups (n=3/group). These mice were subcutaneously injected in the lateral abdomen with tumor cells stably transduced with shNC or shPRTN3 (200 µL; 1×10^6 cells/mL), and tumor growth was then monitored. Tumor width and length were measured once per week, with the tumor volume being calculated as follows: 1/2 (length × width^2). Four weeks later, after a comatose state was induced through inhalation of ethyl ether, mice were sacrificed via dislocation of their cervical vertebrae. Tumors were harvested for qRT-PCR and Western blotting analyses, weighing and photographing were completed. Animal experiments were performed under a project license (No. 2024KT158) granted by Animal Ethics Committee of Nantong University, in compliance with national guidelines for the care and use of animals. A protocol was prepared before the study without registration.

Flow cytometry analyses

Cell cycle distributions and apoptotic death were analyzed for AGS cells and BGC-823 cells with flow cytometry-based approach. After AGS cells and BGC-823 cells (2×10^5–1×10^6 cells) were collected using 0.25% trypsin (cat. no. 25200114; Gibco, Thermo Fisher Scientific, Waltham, MA, USA) and washed once with phosphate-buffered saline (PBS) (1×), they were placed in 1 mL of DNA staining solution (cat. no. CCS012A; MultiSciences, Hangzhou, China) with 10 µL of permeabilization reagent (cat. no. CCS012B; MultiSciences), mixed for 5–10 s, incubated (room temperature, 30 min), and analyzed via flow cytometry (cat. no. 661759; BD Biosciences, Gaithersburg, MD, USA) to determine cell cycle progression. The resulting data were then processed using ModFit LT 5.0 (Verity Software House, Topsham, ME, USA).

For analyses of apoptosis, AGS cells and BGC-823 cells were harvested and rinsed with cold PBS, and $(1–10)\times10^5$ cells were added to diluted binding buffer (cat. no. AP-100-B; MultiSciences), after which 5 µL of Annexin V-allophycocyanin (APC) (cat. no. AP107-100-AVA; MultiSciences) and 10 µL of propidium iodide (cat. no. AP107-100-PI; MultiSciences) were added to each tube. Cells were then shaken gently, which was followed by a room temperature incubation for 5 min, with flow cytometry then being used to analyze apoptosis. Finally, the resulting data were processed using FlowJo Software v.10.8.1 (Herzenberg Laboratory at Stanford University).

TMA establishment and immunohistochemical staining

The 47 GC patient tumor samples were used to construct a TMA, with immunohistochemical staining being performed as described elsewhere (12). Sections of tissue were stained with anti-PRTN3 (1:3,000; cat. no. AB133613; Abcam) at 4 ℃ for 16 hours and then probed with enzyme-conjugated anti-rabbit IgG (1:10,000; cat. no. 66467-1-Ig; Proteintech), which was followed by imaging with a fluorescence microscope (E200 POL; Nikon). Two pathologists examined random fields of view in all tumor sections.

To calculate PRTN3 positivity, the proportion of cells stained positive for PRTN3 and the intensity of staining were quantified. Positive cells were scored according to the following scheme: 0, 0–10%; 1, 11–50%; 2, 51–80%; and 3, 81–100%. Meanwhile, intensity scoring was performed as follows: 0, negative; 1, weak; 2, medium; and 3, strong. Final PRTN3 expression levels were determined by multiplying the two scores together, with 0–3 points being classified as low and 4–8 points as high.

Statistical analysis

SPSS 19.0 (IBM Corp., Armonk, NY, USA) was used for data analyses, with results shown as the mean ± standard deviation (SD). Differences between two groups were assessed with *t*-tests, and analysis of variance (ANOVA) was used to analyze differences between multiple groups. Logistic regression models were used to determine the correlations between PRTN3 levels and clinicopathologic factors. A P value <0.05 indicated a statistically significant difference.

Results

Characterization of PRTN3 expression and the clinicopathological correlates in GC

When 20 paired GC and paracancerous tissue samples were examined via qRT-PCR and Western blotting, both messenger RNA (mRNA) and protein levels of PRTN3 were found to be upregulated in GC tumors (*Figure 1A,1B*). Consistent with this, immunohistochemical staining of the 47 paired GC and paracancerous tissues in the TMA demonstrated a significantly elevated expression of PRTN3 levels in 25 out of the 47 tissue samples. However, only 15 out of the 47 adjacent tissue samples have shown a significantly elevated expression of PRTN3.

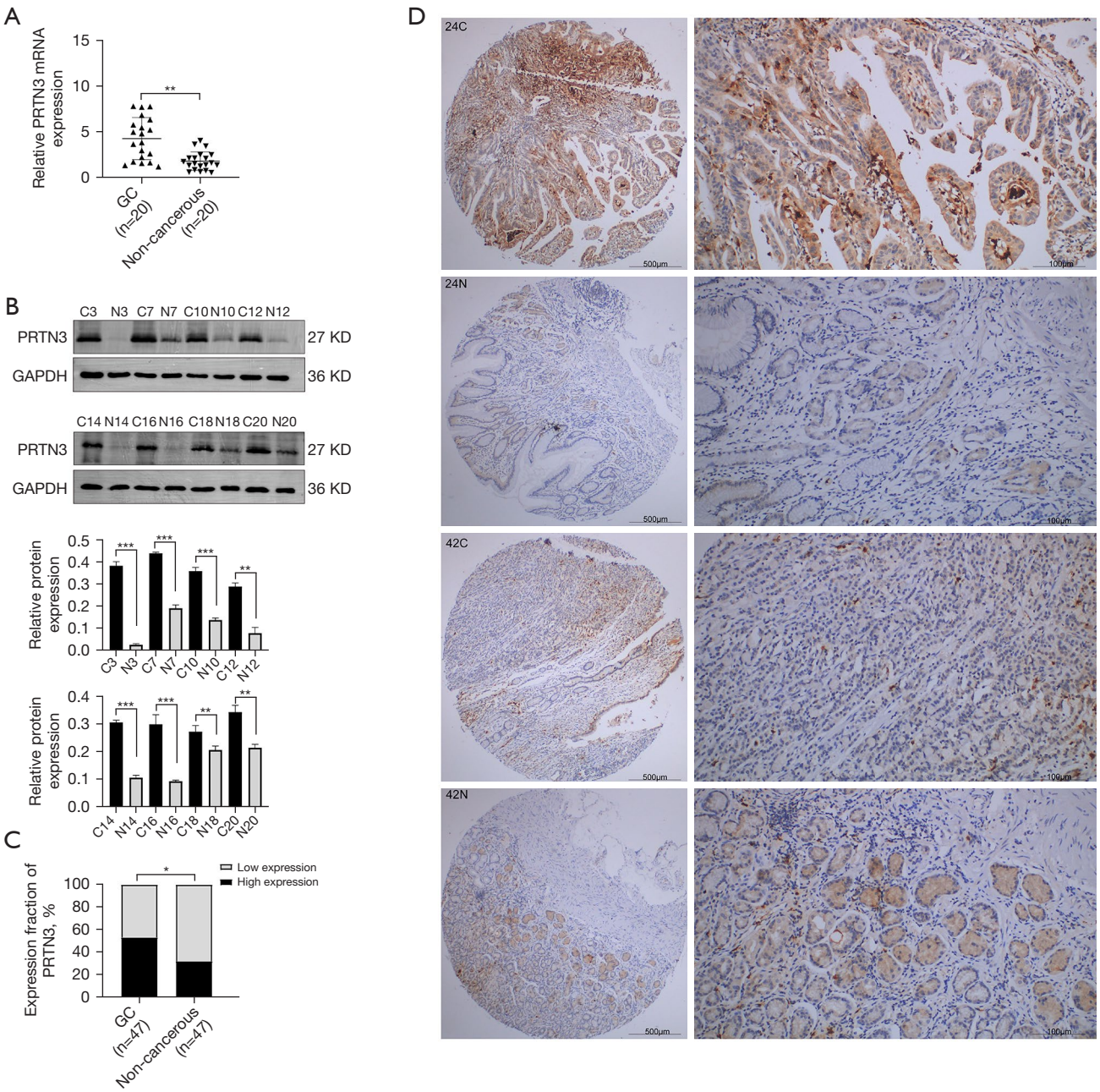

Figure 1 PRTN3 mRNA and protein levels in GC tissue samples. (A,B) PRTN3 mRNA and protein levels in 20 paired GC and paracancerous tissues was detected via qRT-PCR and Western blotting. C and N respectively denote cancerous and noncancerous tissues. (C) Immunohistochemical analysis of PRTN3 levels in 47 paired GC and paracancerous tissues in the tissue microarray. (D) Representative images of the levels of PRTN3 in two paired samples of GC and paracancerous tissue (left scale bar: 500 μm; right scale bar: 100 μm). Staining was done using hematoxylin reagent and observation was done with fluorescence microscope. Data are the mean ± standard deviation. *, P<0.05; **, P<0.01; ***, P<0.001. GC, gastric cancer; PRTN3, proteinase 3; GAPDH, glyceraldehyde-3-phosphate dehydrogenase; mRNA, messenger RNA; qRT-PCR, quantitative real-time reverse transcription polymerase chain reaction.

Table 1 Associations between PRTN3 levels and clinicopathological features in GC cases

Clinicopathological characteristics	N	Low expression, n (%)	High expression, n (%)	χ^2	P value
Gender				0.171	0.75
Male	35	17 (48.6)	18 (51.4)		
Female	12	5 (41.7)	7 (58.3)		
Age (years)				0.521	0.56
≤67	24	10 (41.7)	14 (58.3)		
>67	23	12 (52.2)	11 (47.8)		
Tumor differentiation				0.994	0.39
Low	22	12 (54.5)	10 (45.5)		
Moderate + high	25	10 (40.0)	15 (60.0)		
Tumor diameter (cm)				1.707	0.25
≤4	23	13 (56.5)	10 (43.5)		
>4	24	9 (37.5)	15 (62.5)		
T stage				0.091	>0.99
T1 + T2	16	7 (43.8)	9 (56.3)		
T3 + T4	31	15 (48.4)	16 (51.6)		
N stage				5.379	0.04*
N0 + N1	28	17 (60.7)	11 (39.3)		
N2 + N3	19	5 (26.3)	14 (73.7)		
Tumor localization				1.544	0.24
Upper + middle	17	10 (58.8)	7 (41.2)		
Lower	30	12 (40.0)	18 (60.0)		
TNM stage				0.578	0.56
I + II	25	13 (52.0)	12 (48.0)		
III	22	9 (40.9)	13 (59.1)		

*, P<0.05. PRTN3, proteinase 3; GC, gastric cancer; N, number; TNM, tumor-node-metastasis.

This demonstrates a significantly higher overall degree of PRTN3 expression in GC tissues (*Figure 1C*). When histopathological GC tissue sections were analyzed, PRTN3 expression was primarily restricted to the cytosol (*Figure 1D*).

When clinical parameters from these same 47 patients were analyzed to determine their relationships with the protein levels of PRTN3 using the chi-square method, PRTN3 levels were observed to be significantly correlated only with N stage (P=0.04), but not with age, sex, tumor site, T staging, tumor-node-metastasis (TNM) staging, tumor differentiation, or tumor diameter (*Table 1*).

PRTN3 silencing inhibited in vitro GC cell growth

The significance of PRTN3 in GC was assessed by initially evaluating its levels in different GC cell lines and in normal GES-1 cells. Significantly higher PRTN3 mRNA and protein expression was noted in AGS cells and BGC-823 cells relative to GES-1 cells as determined via qRT-PCR and Western blotting (*Figure 2A*). Therefore, we selected AGS cells and BGC-823 cells with high expression of PRTN3 as cell lines for subsequent cell biology experiments. Three lentiviruses encoding shRNAs

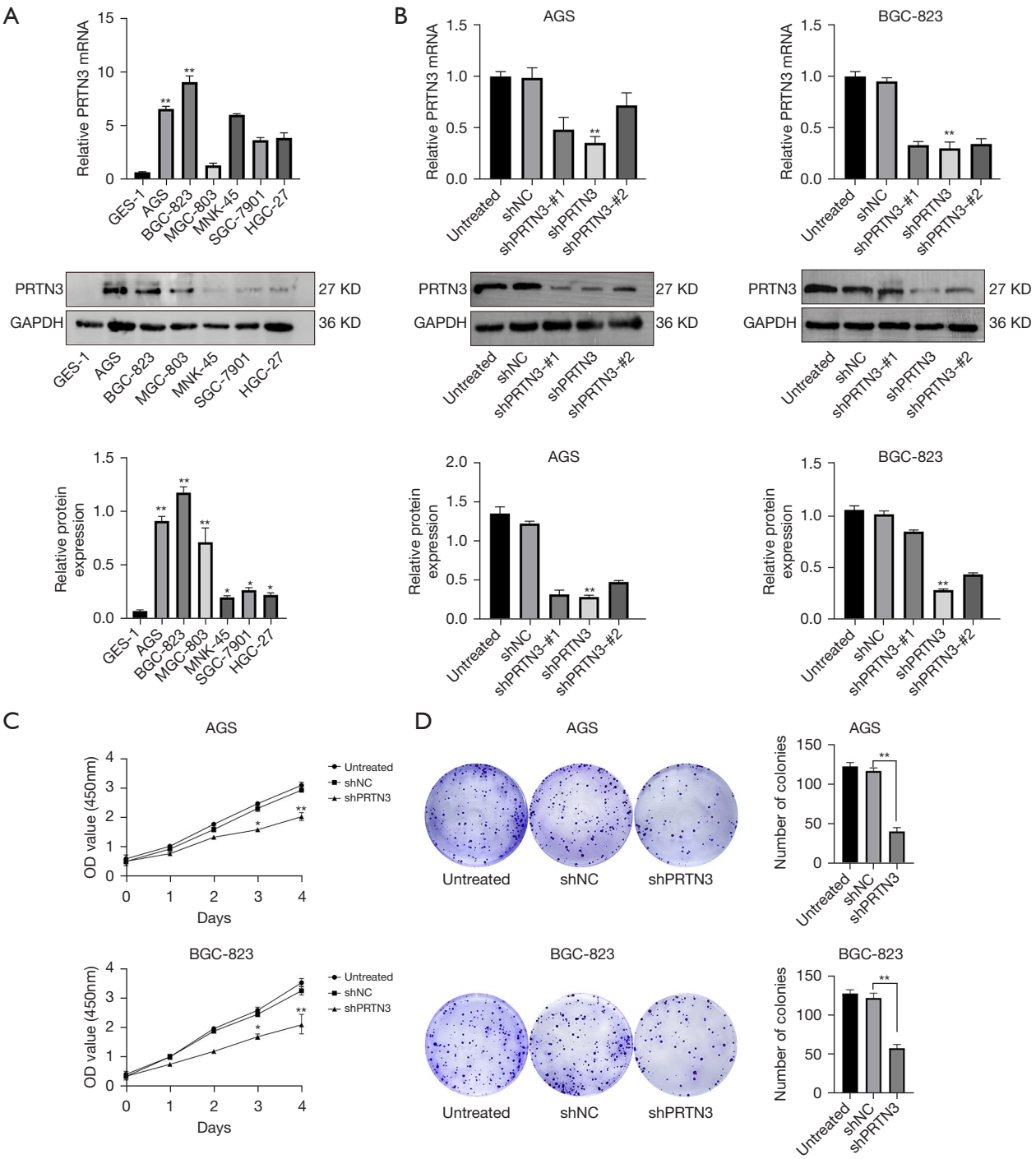

Figure 2 PRTN3 silencing suppressed GC cell proliferation. (A) PRTN3 levels in GC cells were evaluated via qRT-PCR and Western blotting. (B,C) Efficiency of PRTN3 knockdown in lentivirus-transduced AGS cells and BGC-823 cells as assessed by qRT-PCR and Western blotting. (C) CCK-8 and (D) colony formation (were used to assess cell proliferation after transduction with the indicated constructs). Staining was done using crystal violet stain and observation was done using a microscope. Data are the mean ± standard deviation. *, P<0.05; **, P<0.01. PRTN3, proteinase 3; mRNA, messenger RNA; GAPDH, glyceraldehyde-3-phosphate dehydrogenase; shNC, negative control short hairpin RNA; OD, optical density; GC, gastric cancer; qRT-PCR, quantitative real-time reverse transcription polymerase chain reaction; CCK-8, Cell Counting Kit-8.

targeting PRTN3 were then established (shPRTN3-#1, shPRTN3, and shPRTN3-#2), as well as a negative control vector (shNC), and these constructs were transduced into both AGS cells and BGC-823 cells. Successful PRTN3 downregulation was confirmed in these cells via qRT-PCR and Western blotting relative to control cells, with shPRTN3 shRNA being selected for subsequent use, as it possessed the lowest expression of this target (*Figure 2B*).

The effect of PRTN3 on GC cell growth was assessed via CCK-8 assays. Following PRTN3 silencing, AGS cells and BGC-823 cells exhibited markedly lower proliferation rates as compared to control cells (*Figure 2C*). In line with this finding, PRTN3 silencing was associated with a reduction in colony-forming activity (*Figure 2D*).

Silencing PRTN3 suppressed cell cycle progression and promoted GC cell apoptosis

The biological functions of PRTN3 and their effects on cell cycle progression and apoptosis were further examined through a flow cytometry-based approach. When the expression of PRTN3 was downregulated in AGS cells and BGC-823 cells, the proportion of cells in S phase was significantly reduced. Concurrently, the proportions of cells in G0/G1 and G2/M phase were significantly increased (*Figure 3A*). PRTN3 thus appeared to contribute to cell cycle regulation. Consistently, PRTN3 knockdown led to a reduction in CDK4, CDK6, and cyclin D1 levels in both cell lines (*Figure 3B*).

The effect of PRTN3 silencing as a pro-apoptotic factor was assessed via flow cytometry, and an enhanced level of apoptosis was observed following the knockdown of PRTN3 relative to that in control cells (*Figure 3C*). Western blotting was also used to assess apoptosis-related proteins, revealing significantly lower Bcl-2 levels and Bax upregulation at the protein level in both the AGS and BGC-823 cell lines relative to control cells following PRTN3 knockdown (*Figure 3D*).

PRTN3 silencing inhibited in vivo GC tumor growth

To gain insight into how PRTN3 expression affects the *in vivo* growth of GC tumors, a murine xenograft model was established, and the effects on tumor formation were assessed. Markedly reduced tumor weights and volumes were noted in the shPRTN3 group relative to those in controls (*Figure 4A*,*4B*), consistent with the *in vitro* results. Moreover, qRT-PCR and Western blotting confirmed that PRTN3 mRNA and protein levels were reduced in these shPRTN3 tumors relative to those in controls (*Figure 4C*,*4D*).

Discussion

GC is a common malignancy and has been linked with a variety of risk factors, including *Helicobacter pylori*, genetic factors, metabolic disorder, and habits such as alcohol consumption and smoking (15-19). Furthermore, in the field of molecular biology, several serine proteinases have been associated with GC progression (20,21). In this study, the function of PRTN3 in GC was investigated and the potential regulatory mechanisms examined. This can offer a theoretical basis for further exploration of novel diagnostic and therapeutic applications for GC.

The serine protease PRTN3 has functional associations with solid and hematological cancers. For instance, PRTN3 is active specifically within myeloid cells in pediatric acute leukemia and data suggest its role in the pathogenesis of the disease, as well as target for its treatment (22). PRTN3 overexpression in t (8; 21) (q22; q21) acute myeloid leukemia has been linked to chemosensitivity and may hold value as a disease stratification biomarker (23). PRTN3 may be a prognostic signature associated with methylation in clear-cell renal cell carcinoma (RCC), regulating tumorigenic behavior in RCC cells, and thus serve as a possible target and biomarker for this cancer (24). In addition to that, PRTN3 has been proven to be an inflammatory neutrophil-derived factor that can maintain tumor-promoting bacterial growth in squamous extracellular genital cancer and thus has been advanced as a therapeutic target (25). *Clostridium nucleatum* can enhance esophageal cancer growth rates through increases in PRTN3 expression and the activation of PI3K/AKT signaling (26). This factor may thus offer value as a biomarker for early screening aimed at diagnosing and treating esophageal cancer. One study indicated that PRTN3 was highly expressed in pancreatic cancer, where it was associated with lower survival (27).

Although PRTN3 levels have been reported to be elevated in early GC (10), its regulatory mechanism has not been extensively investigated. We hypothesize that PRNT3 is involved in GC progression. Similarly, we discovered in our study that PRTN3 expression was substantially elevated in GC tissues and GC cells, with PRTN3 being mostly present in the cytoplasm of GC cells. It was also found that there was a correlation between PRTN3 and tumor N stage in GC cases. Reduced levels of PRTN3 blocked GC cell growth, as confirmed in both cell experiments and

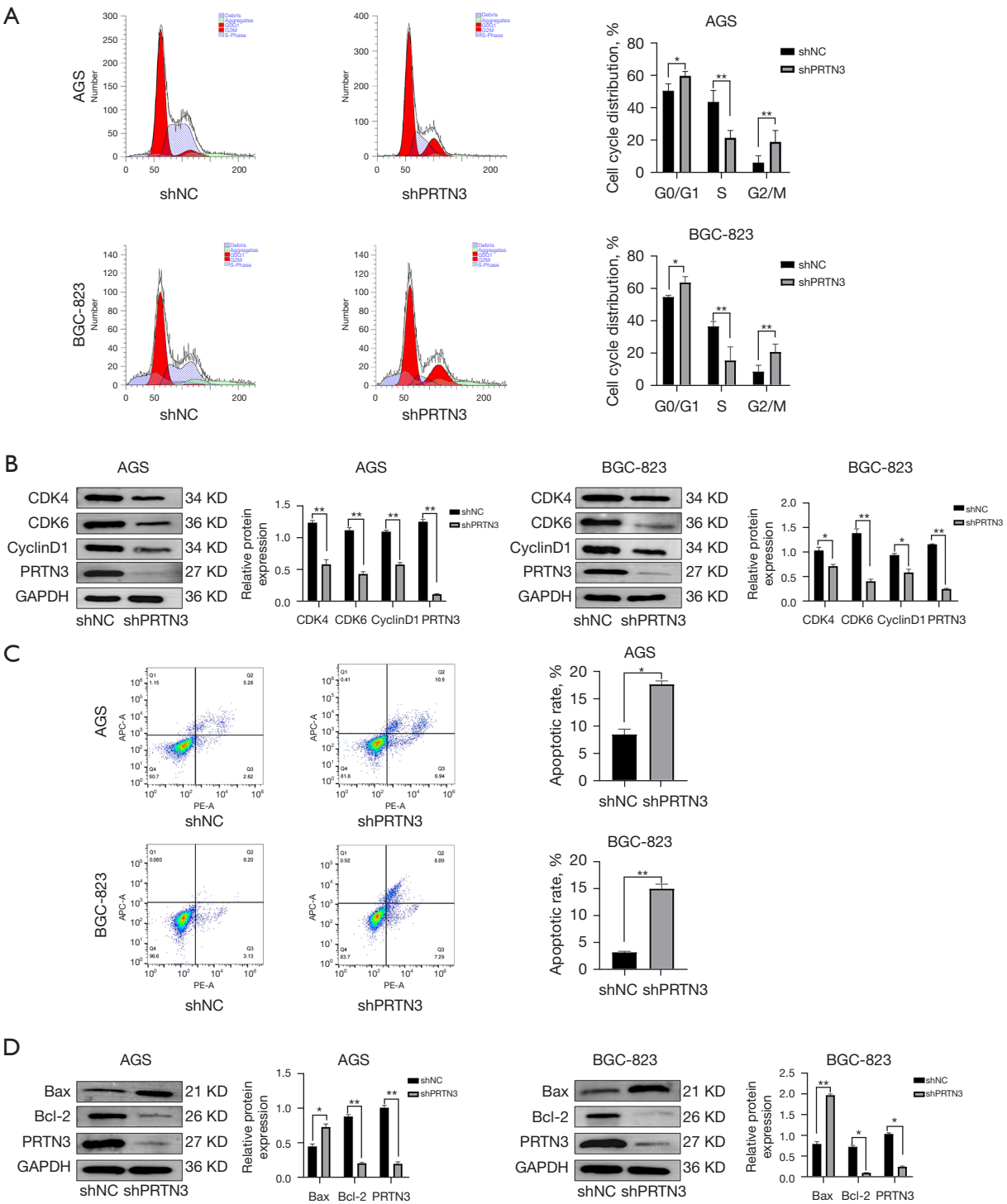

Figure 3 The effect of low PRTN3 levels on the cell cycle and apoptotic death in GC, AGS cells, and BGC-823 cells. (A) FCM analyses of cell cycle distributions with and without PRTN3 silencing. (B) Cell cycle-related protein levels were detected with or without PRTN3 knockdown via Western blotting. (C) FCM analyses of apoptosis with and without PRTN3 silencing. (D) Apoptosis-related protein levels were detected with and without PRTN3 knockdown via Western blotting. Data are the mean ± standard deviation. *, P<0.05; **, P<0.01. shNC, negative control short hairpin RNA; PRTN3, proteinase 3; GAPDH, glyceraldehyde-3-phosphate dehydrogenase; PE, phycoerythrin; APC, allophycocyanin; GC, gastric cancer; FCM, flow cytometry.

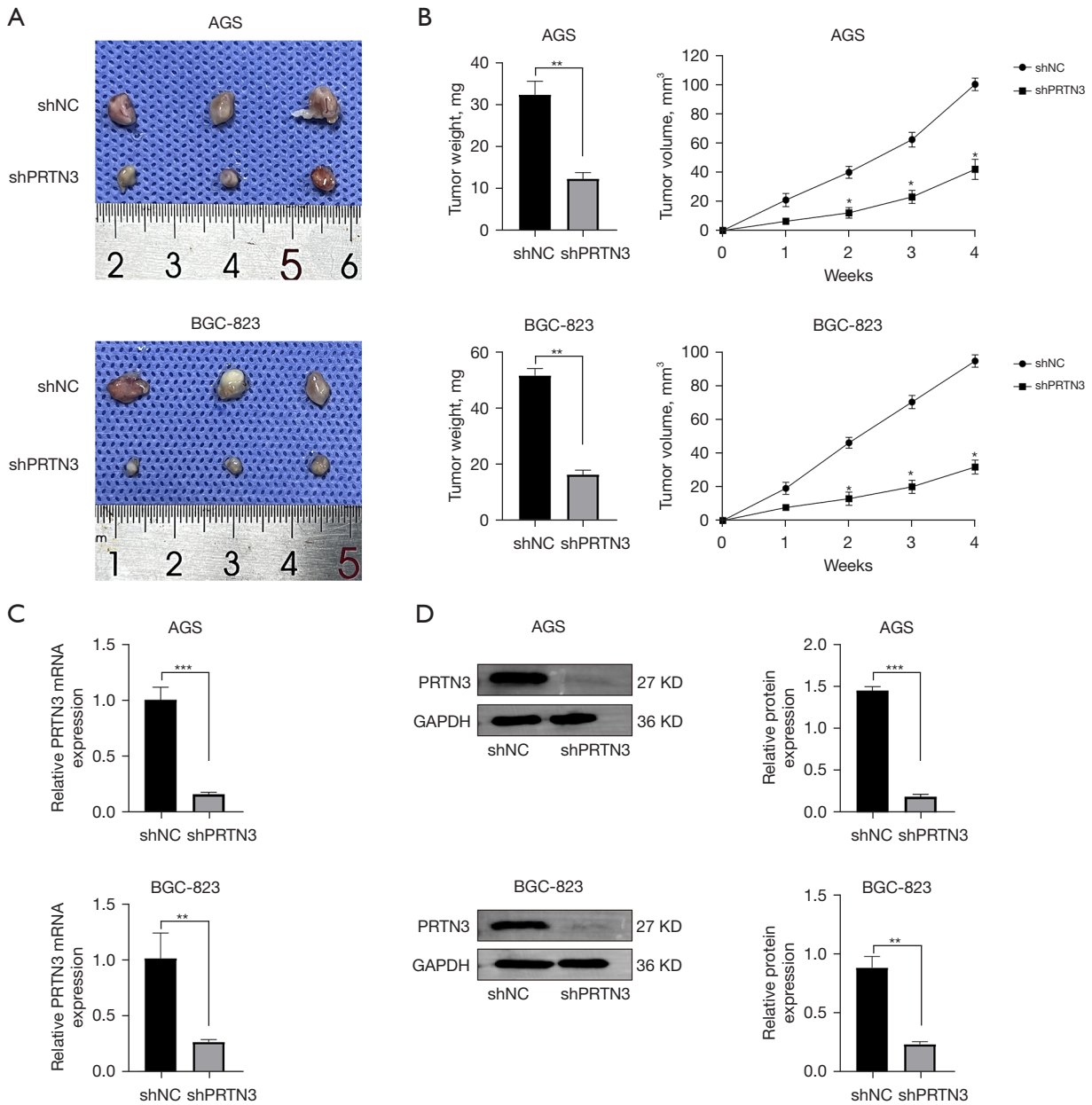

Figure 4 PRTN3 silencing inhibited *in vivo* GC tumor growth. (A,B) Tumor size, weight, and volume were quantified for AGS cells and BGC-823 cells derived from control cells or cells in which PRTN3 was knocked down when transplanted in nude mice. (C,D) PRTN3 mRNA and protein levels in tumors from the indicated mice. Data are the mean ± standard deviation. *, P<0.05; **, P<0.01; ***, P<0.001. shNC, negative control short hairpin RNA; PRTN3, proteinase 3; GAPDH, glyceraldehyde-3-phosphate dehydrogenase; mRNA, messenger RNA; GC, gastric cancer.

mouse models. However, the relationship between PRTN3 and GC prognosis requires further investigation, as does the mechanism underlying PRTN3 regulation of GC progression.

Most tumor types progress in a manner that coincides with the impairment of normal cell cycle and apoptosis-related activity (28). Given the potential links between the turnover of tumor cells and these activities, there are promising opportunities to prevent or treat tumor development by further characterizing their interrelated nature (29). It has been reported that some genes can

regulate tumor progression by affecting the cell cycle and apoptosis. Pectolinarigenin is a compound derived from citrus fruits that can reportedly arrest the cell cycle and induce autophagy and apoptosis in GC cells via the PI3K-AKT-mTOR axis (30). Particular graphene quantum dots can reportedly induce apoptosis and block the cell cycle in estrogen receptor-positive breast cancer cell lines (31). Similarly, INX-315 has been reported to affect tumor progression by inducing cell cycle arrest and senescence in solid tumors (32), and METTL1 may limit breast tumorigenesis by inhibiting cell cycle progression (33). In our study, it was observed that reduced PRTN3 levels blocked the cell cycle and promoted apoptosis in GC cells; furthermore, PRTN3 downregulation was linked to a decrease in the levels of cell cycle-associated proteins including CDK4, CDK6, and cyclin D1, as well as respective reductions and increases in the levels of apoptosis-related Bcl-2 and Bax. The association between PRTN3 and both the cell cycle and apoptosis in GC should be examined to clarify its relevance in the prevention and treatment of this type of cancer.

Tumor invasion and metastatic growth is closely linked to interactions between tumor cells and the extracellular matrix (ECM), angiogenesis, and the epithelial-mesenchymal transition (34). Neutrophils are linked to tumor metastasis and progression (35), and they are also associated with tumor microenvironmental composition, exerting effects in both ECM remodeling and angiogenesis (36). Serine proteases are capable of breaking down the ECM and activating additional proteases related to cancer invasion and are thus involved in GC progression. PRSS2, for instance, is a serine protease that facilitates GC cell spreading, movement, and infiltration (37). PRSS2 is capable of regulating GC cell epithelial-mesenchymal induction and metastatic progression via MMP-9 (38). As a neutral serine protease, PRTN3 is closely associated with neutrophil cluster formation. However, further studies are needed to clarify the role that PRTN3 plays in GC cell migration and invasion in order to elucidate the underlying signaling pathways.

This study demonstrated the regulatory effects of PRTN3 on the growth of GC cells in both cell experiments and mouse models, with flow cytometry indicating that it regulates cell cycle and apoptosis. However, other biological functions of PRTN3 in GC have not been fully elucidated. Clinical data from patients showed that PRTN3 was significantly associated with the N stage of the tumor, although the relationship with other clinical factors needs further verification.

The study involved several limitations which should be mentioned. First, after confirming that the low expression of PRTN3 blocked GC cell proliferation, we did not further verify the effects on migration and invasion of GC cells by inhibiting the expression of PRTN3. Second, the small number of clinical cases did not allow for further investigation of the association between PRTN3 and GC prognosis. We did not collect data on disease-free survival, progression-free survival, or overall survival for the patients included in this study. Finally, the regulatory influence of PRTN3 on pathways associated with GC progression requires further validation. We aim to conduct more basic experiments and further expand the clinical sample size in subsequent studies to achieve a more in-depth exploration of the mechanisms associated with the effects of PRTN3 in GC. Nonetheless, we highlight the need for further pathway analysis and the validation of findings in larger, independent cohorts.

Conclusions

The upregulation of PRTN3 in GC was associated with more advanced tumor N staging. The silencing of PRTN3 was also able to suppress cell cycle progression and growth in GC cells, ultimately stimulating the induction of apoptosis. Efforts to target PRTN3 may thus be of value for the diagnosis and management of this harmful disease.

Acknowledgments

None.

Footnote

Reporting Checklist: The authors have completed the ARRIVE and MDAR reporting checklists. Available at https://tcr.amegroups.com/article/view/10.21037/tcr-2025-153/rc

Data Sharing Statement: Available at https://tcr.amegroups.com/article/view/10.21037/tcr-2025-153/dss

Peer Review File: Available at https://tcr.amegroups.com/article/view/10.21037/tcr-2025-153/prf

Funding: This work was supported by the Nantong Science and Technology Project (No. Jc2023093) and the Nantong

Municipal Health Commission Subject Project (No. MS2022018).

Conflicts of Interest: All authors have completed the ICMJE uniform disclosure form (available at https://tcr.amegroups.com/article/view/10.21037/tcr-2025-153/coif). The authors have no conflicts of interest to declare.

Ethical Statement: The authors are accountable for all aspects of the work in ensuring that questions related to the accuracy or integrity of any part of the work are appropriately investigated and resolved. The study was conducted in accordance with the Declaration of Helsinki (as revised in 2013). The study was approved by the Ethics Committee of Nantong First People Hospital (No. 2024KT182) and informed consent was taken from all the patients. Animal experiments were performed under a project license (No. 2024KT158) granted by Animal Ethics Committee of Nantong University, in compliance with national guidelines for the care and use of animals.

References

1. Smyth EC, Nilsson M, Grabsch HI, et al. Gastric cancer. Lancet 2020;396:635-48.
2. Guan WL, He Y, Xu RH. Gastric cancer treatment: recent progress and future perspectives. J Hematol Oncol 2023;16:57.
3. Ajani JA, D'Amico TA, Bentrem DJ, et al. Gastric Cancer, Version 2.2022, NCCN Clinical Practice Guidelines in Oncology. J Natl Compr Canc Netw 2022;20:167-92.
4. Sung H, Ferlay J, Siegel RL, et al. Global Cancer Statistics 2020: GLOBOCAN Estimates of Incidence and Mortality Worldwide for 36 Cancers in 185 Countries. CA Cancer J Clin 2021;71:209-49.
5. Loison F, Zhu H, Karatepe K, et al. Proteinase 3-dependent caspase-3 cleavage modulates neutrophil death and inflammation. J Clin Invest 2014;124:4445-58.
6. Chen DP, Aiello CP, McCoy D, et al. PRTN3 variant correlates with increased autoantigen levels and relapse risk in PR3-ANCA versus MPO-ANCA disease. JCI Insight 2023;8:e166107.
7. Liu H, Sun L, Zhao H, et al. Proteinase 3 depletion attenuates leukemia by promoting myeloid differentiation. Cell Death Differ 2024;31:697-710.
8. Shi ZR, Duan YX, Cui F, et al. Integrated proteogenomic characterization reveals an imbalanced hepatocellular carcinoma microenvironment after incomplete radiofrequency ablation. J Exp Clin Cancer Res 2023;42:133.
9. Furuya K, Nakajima M, Tsunedomi R, et al. High serum proteinase-3 levels predict poor progression-free survival and lower efficacy of bevacizumab in metastatic colorectal cancer. BMC Cancer 2024;24:165.
10. Guo D, Zhang B, Wu D, et al. Identification of PRTN3 as a novel biomarker for the diagnosis of early gastric cance. J Proteomics 2023;277:104852.
11. Guo Q, Xu J, Huang Z, et al. ADMA mediates gastric cancer cell migration and invasion via Wnt/β-catenin signaling pathway. Clin Transl Oncol 2021;23:325-34.
12. Wang F, Li P, Feng Y, et al. Low expression of RASSF10 is associated with poor survival in patients with colorectal cancer. Hum Pathol 2017;62:108-14.
13. Anagnostopoulos GK, Stefanou D, Arkoumani E, et al. Bax and Bcl-2 protein expression in gastric precancerous lesions: immunohistochemical study. J Gastroenterol Hepatol 2005;20:1674-8.
14. Wang MQ, Chen YR, Xu HW, et al. HKDC1 upregulation promotes glycolysis and disease progression, and confers chemoresistance onto gastric cancer. Cancer Sci 2023;114:1365-77.
15. Tan P, Yeoh KG. Genetics and Molecular Pathogenesis of Gastric Adenocarcinoma. Gastroenterology 2015;149:1153-1162.e3.
16. Tramacere I, Negri E, Pelucchi C, et al. A meta-analysis on alcohol drinking and gastric cancer risk. Ann Oncol 2012;23:28-36.
17. Lordick F, Carneiro F, Cascinu S, et al. Gastric cancer: ESMO Clinical Practice Guideline for diagnosis, treatment and follow-up. Ann Oncol 2022;33:1005-20.
18. Lu L, Mullins CS, Schafmayer C, et al. A global assessment of recent trends in gastrointestinal cancer and lifestyle-associated risk factors. Cancer Commun (Lond) 2021;41:1137-51.
19. Jiang Z, Gu Z, Lu X, et al. The role of dysregulated metabolism and associated genes in gastric cancer initiation

and development. Transl Cancer Res 2024;13:3854-68.
20. Qin H, Zhang S, Shen L, et al. High expression of serine protease 2 (PRSS2) associated with invasion, metastasis, and proliferation in gastric cancer. Aging (Albany NY) 2023;15:2473-84.
21. Qin S, Wang Z, Huang C, et al. Serine protease PRSS23 drives gastric cancer by enhancing tumor associated macrophage infiltration via FGF2. Front Immunol 2022;13:955841.
22. Bories D, Raynal MC, Solomon DH, et al. Down-regulation of a serine protease, myeloblastin, causes growth arrest and differentiation of promyelocytic leukemia cells. Cell 1989;59:959-68.
23. Jiang L, Li XP, Dai YT, et al. Multidimensional study of the heterogeneity of leukemia cells in t(8;21) acute myelogenous leukemia identifies the subtype with poor outcome. Proc Natl Acad Sci U S A 2020;117:20117-26.
24. Wei Z, Wu B, Wang L, et al. A large-scale transcriptome analysis identified ELANE and PRTN3 as novel methylation prognostic signatures for clear cell renal cell carcinoma. J Cell Physiol 2020;235:2582-9.
25. Rustetska N, Szczepaniak M, Goryca K, et al. The intratumour microbiota and neutrophilic inflammation in squamous cell vulvar carcinoma microenvironment. J Transl Med 2023;21:285.
26. Hu D, Ansari D, Zhou Q, et al. Low P4HA2 and high PRTN3 expression predicts poor survival in patients with pancreatic cancer. Scand J Gastroenterol 2019;54:246-51.
27. Lei J, Xu F, Deng C, et al. Fusobacterium nucleatum promotes the early occurrence of esophageal cancer through upregulation of IL-32/PRTN3 expression. Cancer Sci 2023;114:2414-28.
28. Capiod T, Shuba Y, Skryma R, et al. Calcium signalling and cancer cell growth. Subcell Biochem 2007;45:405-27.
29. Soták M, Sumová A, Pácha J. Cross-talk between the circadian clock and the cell cycle in cancer. Ann Med 2014;46:221-32.
30. Lee HJ, Venkatarame Gowda Saralamma V, Kim SM, et al. Pectolinarigenin Induced Cell Cycle Arrest, Autophagy, and Apoptosis in Gastric Cancer Cell via PI3K/AKT/mTOR Signaling Pathway. Nutrients 2018;10:1043.
31. Ku TH, Shen WT, Hsieh CT, et al. Specific Forms of Graphene Quantum Dots Induce Apoptosis and Cell Cycle Arrest in Breast Cancer Cells. Int J Mol Sci 2023;24:4046.
32. Dietrich C, Trub A, Ahn A, et al. INX-315, a Selective CDK2 Inhibitor, Induces Cell Cycle Arrest and Senescence in Solid Tumors. Cancer Discov 2024;14:446-67.
33. Du D, Zhou M, Ju C, et al. METTL1-mediated tRNA m(7)G methylation and translational dysfunction restricts breast cancer tumorigenesis by fueling cell cycle blockade. J Exp Clin Cancer Res 2024;43:154.
34. Wittekind C, Neid M. Cancer invasion and metastasis. Oncology 2005;69 Suppl 1:14-6.
35. Swierczak A, Mouchemore KA, Hamilton JA, et al. Neutrophils: important contributors to tumor progression and metastasis. Cancer Metastasis Rev 2015;34:735-51.
36. Kim J, Bae JS. Tumor-Associated Macrophages and Neutrophils in Tumor Microenvironment. Mediators Inflamm 2016;2016:6058147.
37. Chen Y, Wang B, Zhao Z, et al. PRSS2 overexpression relates to poor prognosis and promotes proliferation, migration and invasion in gastric cancer. Tissue Cell 2022;79:101949.
38. Wang F, Yi J, Chen Y, et al. PRSS2 regulates EMT and metastasis via MMP-9 in gastric cancer. Acta Histochem 2023;125:152071.

(English Language Editor: J. Gray)

Cite this article as: Zhu H, Wang F, Lu X, Wu H, Shi C, Matsas S, Peixoto RD, Aruquipa MPS, Tang C, Feng S. Low expression of PRTN3 regulates the progression of gastric cancer by inhibition of cell cycle and promotion of apoptosis. Transl Cancer Res 2025;14(2):1415-1427. doi: 10.21037/tcr-2025-153